International Scholarly Research Network
ISRN Corrosion
Volume 2012, Article ID 323676, 12 pages
doi:10.5402/2012/323676

Research Article

Porous Layer Characterization of Anodized and Black-Anodized Aluminium by Electrochemical Studies

M. Franco, S. Anoop, R. Uma Rani, and A. K. Sharma

Thermal Systems Group, ISRO Satellite Centre, Indian Space Research Organisation, P.O. Box No. 1795, Old Airport Road, Vimanapura Post Office, Bangalore 560017, India

Correspondence should be addressed to R. Uma Rani, rurani@isac.gov.in

Received 17 September 2012; Accepted 1 November 2012

Academic Editors: H. Altun, G. Marginean, H. Miao, and C. Valentini

Three types of black anodic coatings, namely, black dyeing (BD), inorganic colouring (IC), and electrolytic colouring (EC) were prepared by conventional type II sulphuric acid anodizing on Al6061 alloys. Electrochemical behaviour of these coatings was studied by exposure to 3.5% wt sodium chloride solution for prolonged immersion periods up to 360 hours. The porous layer characteristics of all sealed, fresh and autosealed coatings were investigated by means of electrochemical impedance spectroscopy (EIS). An equivalent circuit that reproduces the a.c. impedance results of porous aluminium oxide films is proposed. The breakpoint frequency and damage function analysis were carried out to analyse the coating's electrochemical behaviour. Corrosion morphology was studied by scanning electron microscopy. It was observed that BD and IC behaved in a very similar manner to sulphuric acid anodising (SAA). However EC was behaving in an entirely different manner. Among all colouring methods BD was showing very less R_p values. All these findings were further confirmed by linear polarisation studies. No major evidence of localised corrosion or pitting of the black anodic coatings was observed in SEM micrographs.

1. Introduction

Black anodic coatings are widely used in space components for various reasons such as passive thermal control of satellites and absorption of stray lights in the optical components. They have the advantages of providing very high corrosion resistance, wear resistance, thermal control properties, and so forth to components made of aluminium alloys. The unique duplex porous structure of the anodic oxide layer formed on the surface of aluminium alloys helps in impregnation of various colouring pigments providing required colour to the components. Variety of black anodizing processes were studied by us for thermal control applications, namely, organic black dyeing, black permanganate conversion coating, inorganic colouring, integral black colouring, electrolytic black colouring, and so forth [1–5]. Hydrothermal sealing (HTS) of the pores after black anodizing is done to avoid penetration of foreign elements into the pores which may deteriorate the resistance to corrosion.

Electrochemical impedance spectroscopy (EIS) has been the most widely used technique to study the porous and barrier layer properties of anodic oxide coatings. Hoar and Wood investigated on dependence of various processing parameters on anodization of aluminium using impedance data [6]. It was established that the barrier layer thickness, pore diameter, and the hexagonal cell dimensions are directly proportional to the anodizing voltage and also depend on the electrolyte type, concentration, and temperature. The porous layer thickness mainly depends on the current density and anodizing time in addition to the general processing parameters [7–9]. The mechanisms of evolution of the porous layer during HTS by dissolution of anhydrous alumina and precipitation of hydrated alumina inside the pores were studied in detail with the help of IR spectroscopy, electron diffraction, and transmission electron microscopy [10–12]. The typical structure of hydrothermally sealed anodic film was identified by Wefers [13, 14].

Equivalent electrical circuit models were developed to fit the experimental impedance data and to estimate the electrochemical parameters of porous and barrier layers [6, 15–28]. Frequencies as low as 1 mHz were used to evaluate the barrier layer resistance and capacitance values from Bode

plots in the aforementioned studies. Mansfeld et al. used porous layer resistance (R_p) to quantify the quality of the sealing [18, 29, 30]. Mechanism of sealing was investigated by Lopez et al. using SEM, TEM, and EIS [31–33]. Effects of other protective coatings on aluminium alloys were also studied and compared with conventional anodizing process [30, 34].

Many investigators used specific admittance A_s, which is the inverse of the impedance at 1000 Hz normalized to the surface area, to measure the quality of the various sealing methods of anodic coatings based on ASTM B457 [24, 35–37]. Breakpoint frequency also renders information regarding the corrosion stability of the coating [29]. Other electrochemical studies using polarisation curves were also used to investigate the influence of sealing methods and autosealing on corrosion of anodic coatings [38, 39].

In the present work investigators focus on the changes occurring in the porous layer during various colouring processes, HTS, and ageing. The range of frequency sweep (0.1 Hz to 30 kHz) was selected in order to investigate on porous layer characteristics. Major changes in the cell walls and barrier layer are not expected and therefore not considered. The effect of different colouring techniques on the electrochemical impedance behaviour and effectiveness of sealing of anodic coatings are less studied, and there is a dearth of literature in this direction. Hence the aim of the authors is to investigate the electrochemical characteristics of porous layer of various black anodic coatings used in the space industry by means of EIS and linear polarisation (LP) techniques.

2. Experimental

The preparation process of black anodic films involved four main consecutive steps: surface pretreatments, anodizing, colouring (black anodizing), and sealing.

Al 6061-T6 alloy (0.8–1.2 wt% Mg, 0.6 wt% Si, 0.15 wt% Mn, 0.28 wt% Cu, 0.7 wt% Fe, reminder Al) of size 35 mm × 25 mm × 4 mm was degreased in trichloroethylene and then alkaline cleaned in sodium carbonate (Na_2CO_3), 20 g L^{-1} and tri sodium orthophosphate ($Na_3PO_4 \cdot 12H_2O$), 25 g L^{-1} operating at 60 ± 5°C for 2-3 minutes. Then it was neutralised in an aqueous solution of sulphuric acid (SG 1.83) 10 mL L^{-1}, hydrofluoric acid (40%) 12.5 mL L^{-1} and nitric acid (SG 1.42) 25 mL L^{-1} operating at room temperature (25 ± 5°C). The samples were rinsed in demineralised water at the end of each step.

The aluminium samples were then anodized using a conventional type II sulphuric acid anodizing technique in 15 wt% sulphuric acid solution in a lead lined tank (as cathode) with air agitation facility at room temperature (25 ± 5°C). Anodising was done at constant voltage mode at 18 V for duration of 20–50 minutes. The samples were then immediately rinsed in distilled water.

The black anodizing was carried out using three different methods, namely, black dyeing, inorganic colouring, and electrolytic colouring as per the process parameters given in Table 1.

Black dyeing (BD) was carried out by immersing the anodised specimens in an organic black dye solution. Inorganic colouring (IC) was done by immersing the anodised specimens in two solutions successively as described in Table 1. Black colour produced is the result of an inorganic reaction between the precursor solutions inside the anodic pores which forms cobalt sulphide (CoS) which renders black colour to the sample [2]. Electrolytic colouring (EC) was carried out in an electrolyte containing $SnCl_2$ by applying 20 V AC for 15 minutes. This is primarily an AC electrodeposition technique where metallic salts are deposited within the anodic porous layer [40]. Lead was used as the counterelectrode for the process.

Hydrothermal sealing was done by immersing the samples in boiling demineralised water for 30 minutes after each black anodizing process for all the specimens. A set of unsealed samples were also prepared for investigating the effect of autosealing on the corrosion behaviour of black anodic coatings. The samples were preserved for six months before carrying out corrosion experiments.

The thickness of anodic films was measured using Fischer Isoscope thickness meter which works on the principle of eddy current.

Electrochemical impedance spectroscopy (EIS) was employed to monitor the corrosion behaviour of the anodised specimens. It was performed using a frequency response analyser (Autolab PGSTAT 302N, Eco-chemie, The Netherlands) driven by Nova 1.4 software. A typical three-electrodes cell, Ag/AgCl (saturated with KCl) as reference electrode, a platinum rod as counterelectrode, and the specimen as the working electrode (1 cm^2 exposed area) were used in the cell. All the electrochemical tests were conducted in an unstirred, neutral 3.5 wt% sodium chloride solution at room temperature. Prior to test, the anodised samples in sealed condition were subjected to 10 min, 5, 24, 30, 120, 264, and 360 hrs of immersion in 3.5 wt% sodium chloride solution to simulate the prolonged/accelerated exposure. The EIS tests were performed with a sinusoidal AC amplitude signal of 10 mV over the open circuit potential (OCP) in the frequency range from 30 kHz to 0.1 Hz.

Linear polarisation tests were also conducted on test specimens for initial immersion and after final immersion period (up to 360 hours) to verify the corrosion results of anodic coatings obtained by EIS, using Nova 1.4 software in the same instrument (Autolab PGSTAT 302N, potentiostat/galvanostat, The Netherlands). The tests were performed at a scan rate of 1 mVs^{-1} in the applied potential range of −0.250 V to +0.250 V with respect to OCP.

The surface morphology of corrosion test samples was examined with SEM (LEICA S. 400 I, Cambridge, UK) to analyse the extent of corrosion on the sample surfaces after immersion in the corrosive medium.

3. Results and Discussions

Thickness of anodic and black anodic coatings was found in the range of 18–20 μm using Fischer Isoscope thickness meter.

Table 1: Black anodizing process parameters.

Sl. no.	Process	Concentrations	Process parameters
1	Black dyeing	Jet black—11 g L^{-1}	pH = 5 ± 0.5
		(Commercial organic black dye procured	75 ± 5°C
		from Khatau Valabhdas, Gujarat, India)	15 min
2	Inorganic colouring	Step 1:	25 ± 5°C
		Cobalt acetate, $Co(C_2H_3O_2)_2$—200 g L^{-1}	15 min
		Step 2:	25 ± 5°C
		Ammonium sulphide, $(NH_4)_2S$—25 mL L^{-1}	15 min
3	Electrolytic colouring	Sulphuric acid, H_2SO_4—10 mL L^{-1}	pH = 1.1 ± 0.3
		Stannous chloride, $SnCl_2$—20 g L^{-1}	25 ± 5°C
		Phenol sulphonic acid—10 mL L^{-1}	Voltage ~20 V, AC
			15 min

* Each step was followed by demineralized water rinsing.

3.1. Electrochemical Impedance Spectroscopy. The experimental electrochemical results of anodized samples are very similar to those measured by other research groups working on similar anodised and sealed aluminium samples [29–39].

The bode plots for sealed anodic and black anodic coatings are shown in Figures 1–4. The bode-modulus plots of BD, IC, and SAA clearly show the three typical regions of a properly sealed anodic oxide coating [15]. The higher impedance values at frequencies (f) ≤ 1 Hz clearly point to the barrier layer characteristics of the anodic coating. Evaluation of barrier layer parameters required measurement at lower frequencies and was not considered as it is beyond the scope of this work. The quasi-horizontal region in the bode-modulus plot (where the impedance is virtually independent of frequency) and the corresponding minima region in the bode-phase plot represent the resistive behaviour of the porous layer. The steep portion towards the higher frequency in the bode-modulus plot represents the capacitive behaviour of the porous layer [15, 18]. These parameters render useful information related to the hydration reactions within the pores [31–33].

The impedance spectra of anodic and black anodic coatings in the low-frequency region are found to be identical over the entire immersion period up to 360 h, revealing the compact and stable nature of the barrier layer. There is no evidence of penetration of the solution through the barrier layer. At intermediate and higher-frequency regions the impedance spectra exhibit variations which is indicative of the instability of the porous layer towards the action of electrolyte. Initially the resistive segment falls on immersion up to 24 h and then rises on extended immersion upto 360 h as evident from Figures 1(a), 2(a), and 3(a). This is also substantiated by the shifts of phase-angle minima towards the high-frequency region during initial immersion and then to the low-frequency region after 24 h of immersion as shown in Figures 1(b), 2(b), and 3(b). This phenomenon was explained using pore wall dissolution, gel condensation, and hydrated alumina precipitation mechanism [31, 32]. During hydrothermal sealing the pores were filled with sealing solution which plugs the pore mouths by the formation of acicular boehmite and compact intermediate layers at the expense of dissolving anhydrous alumina from the coating surface and the pore walls. The major stage of pore widening essentially happens during the initial immersion period in the sodium chloride solution which results in the decrease of porous layer resistance. The porous anodic film is predominantly attacked by the aggressive ions leading to enhanced conductive paths, and at the same time the precipitation of hydrated alumina is retarded due to this aggressive action of chloride ions [39]. The fall of the quasi horizontal section in the bode-modulus and right shift of phase-angle minima in the bode-phase is essentially attributed to this phenomenon. On further immersion, the dissolved anhydrous alumina from around the pore wall reacts with the absorbed water resulting in the formation of voluminous hydrated alumina. This precipitation of hydrated alumina in the form of bayerite ($Al_2O_3 \cdot 3H_2O$), a trihydrate that is stable in ambient temperature, plugs the entire pore length, resulting in the self-sealing of the pores on ageing [31, 39]. This explains the raise in the resistive portion of the impedance spectra and displacement of phase-angle minima towards the lower-frequency region after 24 h of immersion (Figures 1–3). The results are consistent with the mechanism of self-sealing proposed by Lopez et al. and Zuo et al. [31, 38]. It is interesting to note that the spectra obtained after 360 h of immersion are almost identical to those of 10 min immersion. This might be due to the saturation of the entire pore length with the precipitation of hydrated alumina at this stage. The two-time constants still remain up to 360 h of immersion.

A closer analysis of the BD impedance spectra reveals that, after the initial exposure of 5 h a drastic decrease of porous layer resistance is observed as the quasi-horizontal region shifts downward in the bode-modulus plot. This could be attributed to an unstable black dyed porous layer which was degraded by the electrolytic attack. On further immersion an increase in R_p is observed similar to that of SAA samples owing to the self-sealing mechanism as discussed earlier. It is also validated by the fact that the phase-angle minima are shifted to a high-frequency side in the bode-phase plot (Figure 2(b)) in the initial exposure

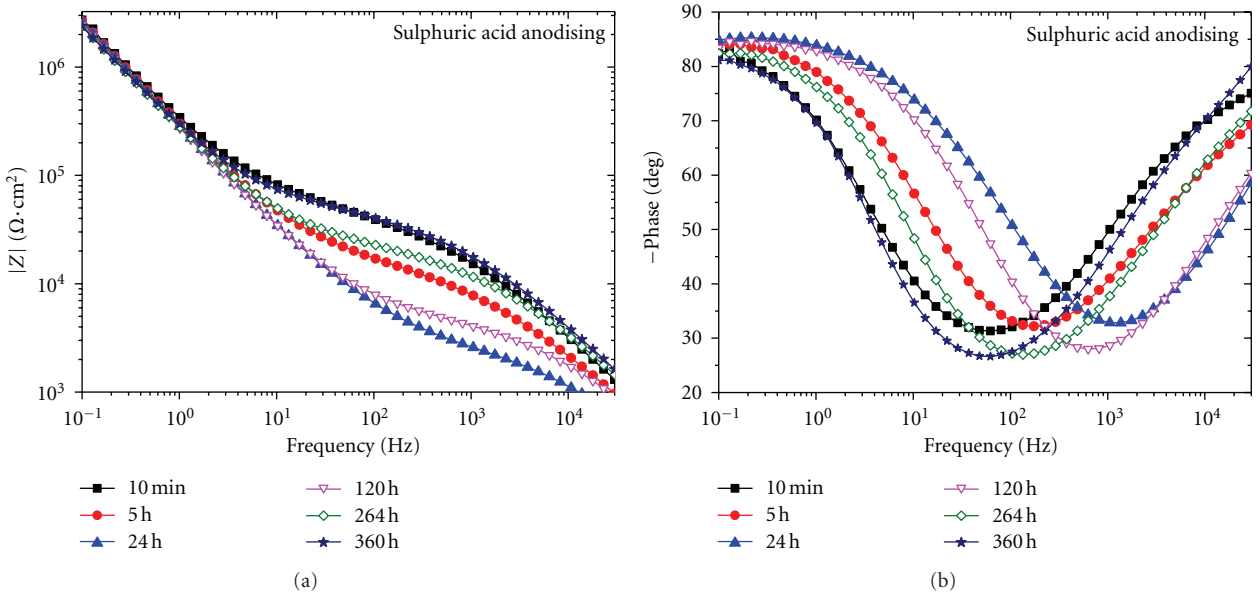

Figure 1: Bode plots for sulphuric acid anodized and sealed Al 6061 for prolonged immersion in 3.5 wt% NaCl. (a) Bode-modulus. (b) Bode-phase.

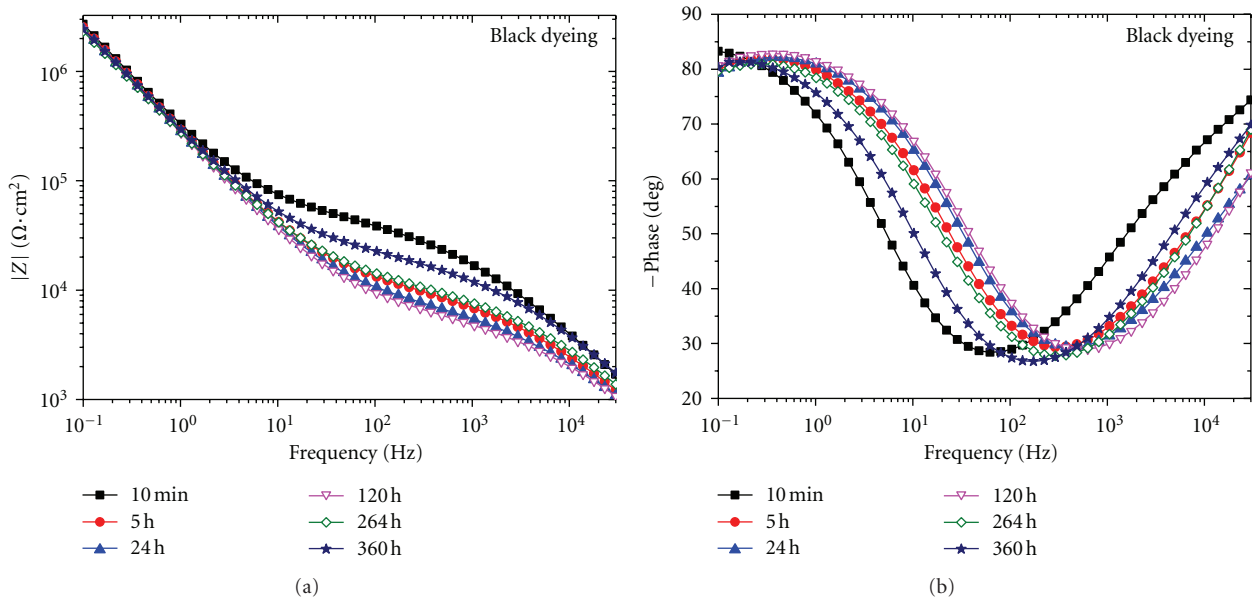

Figure 2: Bode plots for anodized and black dyed (sealed) samples for prolonged immersion in 3.5 wt% NaCl. (a) Bode-modulus. (b) Bode-phase.

and over long periods of immersion the minima shifted back towards the low-frequency side. However the spectral region corresponding to barrier layers is found to be identical throughout the immersion period indicating a highly stable and unaffected barrier layer. The porous layer resistances for various immersion periods for BD are found to be lowest compared to other colouring samples. This shows that black dye technique was unable to produce a stable corrosion-resistant porous layer compared to IC and SAA.

However, the quasi-horizontal region of the bode-modulus plot for IC specimens is relatively higher and shifted towards a lower-frequency side which can be attributed to a better porous layer resistance compared to SAA and BD. The identical slopes (i.e., capacitance values) at low-frequency ($f \leq 1$ Hz) and at high-frequency ($f \geq 10$ kHz) regions of bode-modulus plot indicate the unaltered porous and barrier layers. Slight shifts of phase-angle minima towards the low-frequency region indicate an increase in the porous layer resistance over extended immersion periods as shown in Figure 3(b). The self-sealing mechanism of precipitation of the bayerite throughout the length of the pore is assumed to be enhancing the porous layer resistance over prolonged

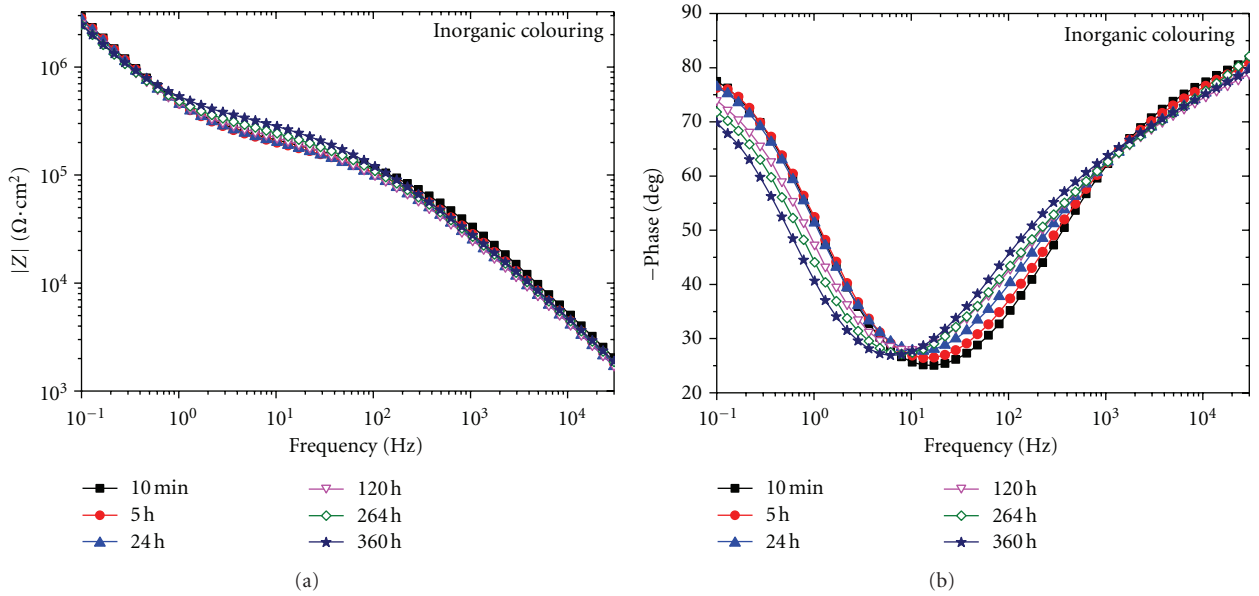

Figure 3: Bode plots for anodized and inorganic coloured (sealed) samples for prolonged immersion in 3.5 wt% NaCl. (a) Bode-modulus. (b) Bode-phase.

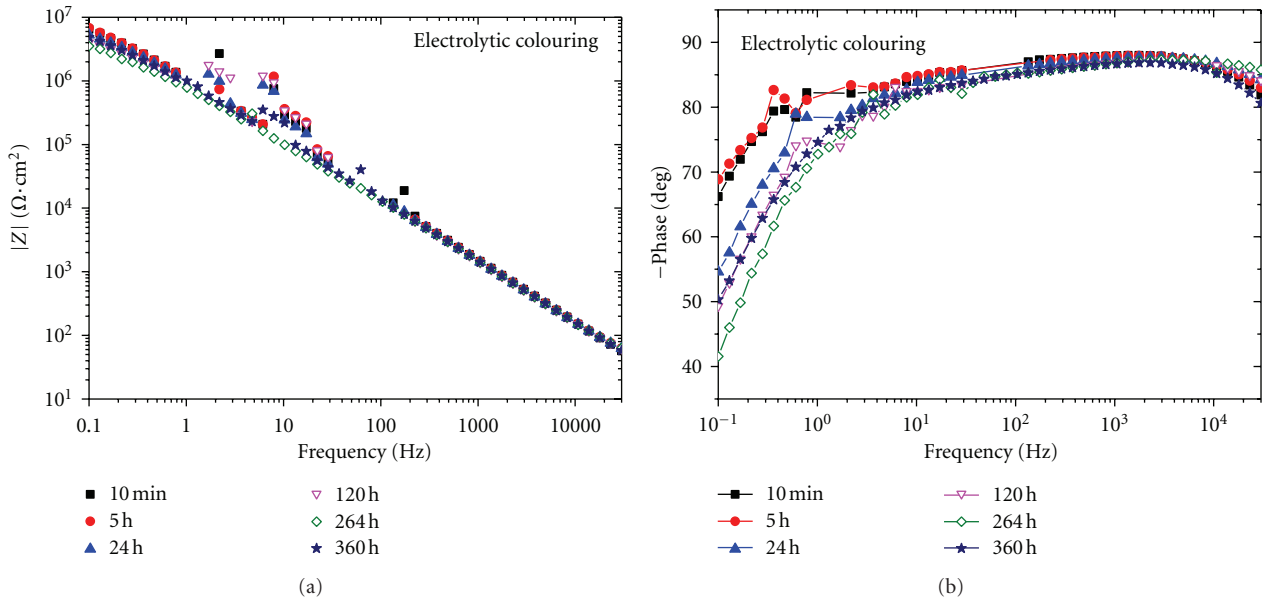

Figure 4: Bode plots for anodized electrolytic coloured (sealed) samples for prolonged immersion in 3.5 wt% NaCl. (a) Bode-modulus. (b) Bode-phase.

immersion. Overall the spectra for all the immersion periods remain almost identical indicating very good stability of the coating produced by inorganic colouring technique.

Interestingly, the impedance spectra for EC specimens as shown in Figure 4 are found to be entirely different from other black anodic coatings. The spectra show a single straight line for the complete frequency range rather than the three typical regions of a properly sealed anodic film. There is no significant change in the impedance spectra even after an extended immersion period of 30 hours. A raise of impedance values at low frequencies ($f \leq 1$ Hz) compared to other samples could be an indication of barrier layer thickening as explained by Tsangaraki-Kaplanoglou et al. [40]. This is mainly due to the application of an a.c. voltage (~20 V) higher than that of conventional anodizing voltage. In this process an electrodeposition of tin occurs on the surface of the anodic oxide layer during the cathodic half cycle, and levelling up of the pores happens during the other half. The deposited crystalline β-tin (100) of grain size 20–40 nm essentially brings the required colour to the coating

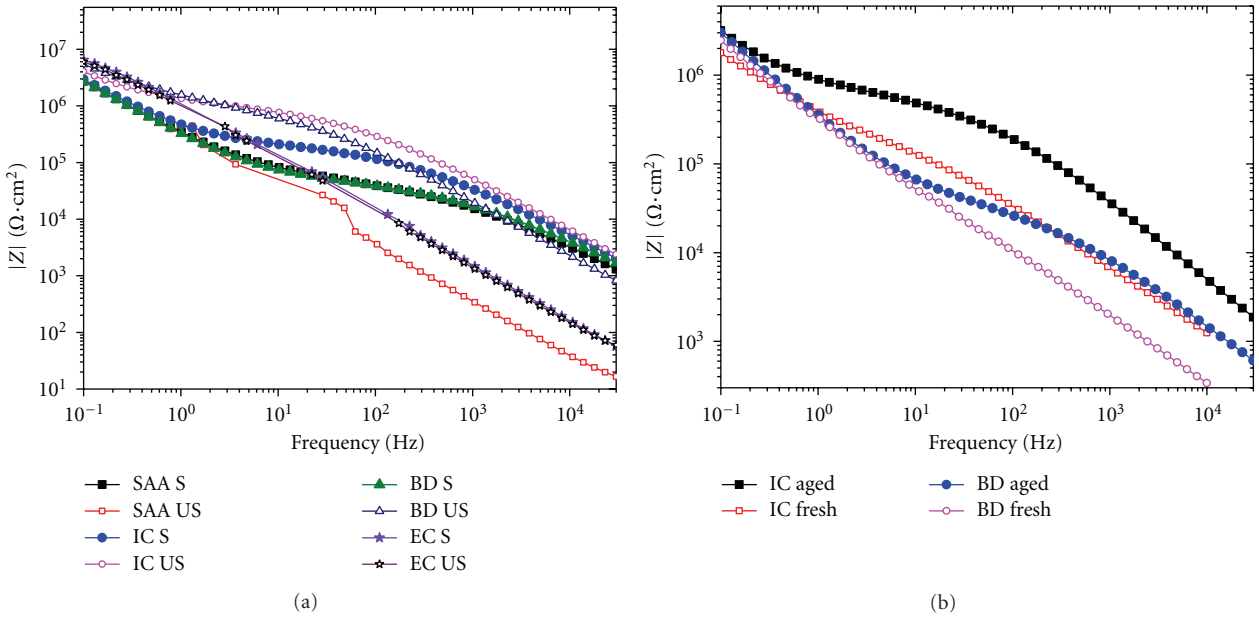

Figure 5: Bode-modulus plots showing variation of (a) hydrothermal sealing against unsealed samples and (b) autosealing/ageing of unsealed samples after 6 months of atmospheric exposure. "S" and "US" indicate "sealed", and "unsealed", respectively.

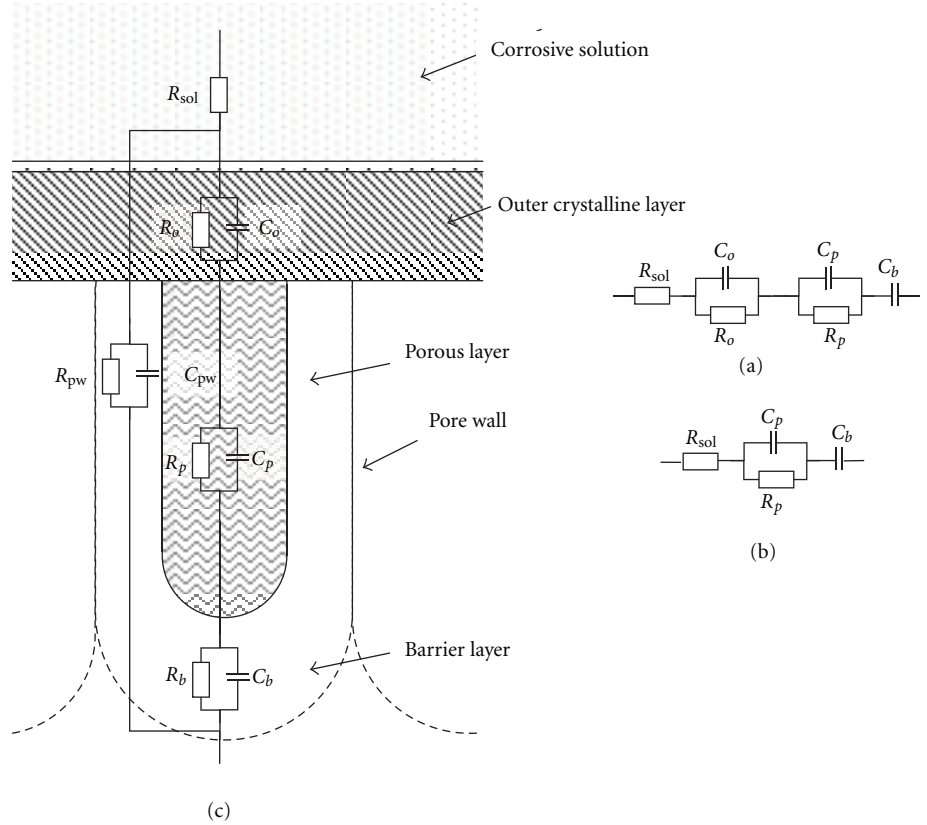

Figure 6: (a) Equivalent circuits for fitting impedance data of sealed coating, (b) equivalent circuits for fitting impedance data of electrolytic colouring, and (c) physical significance of various electrochemical fit parameters.

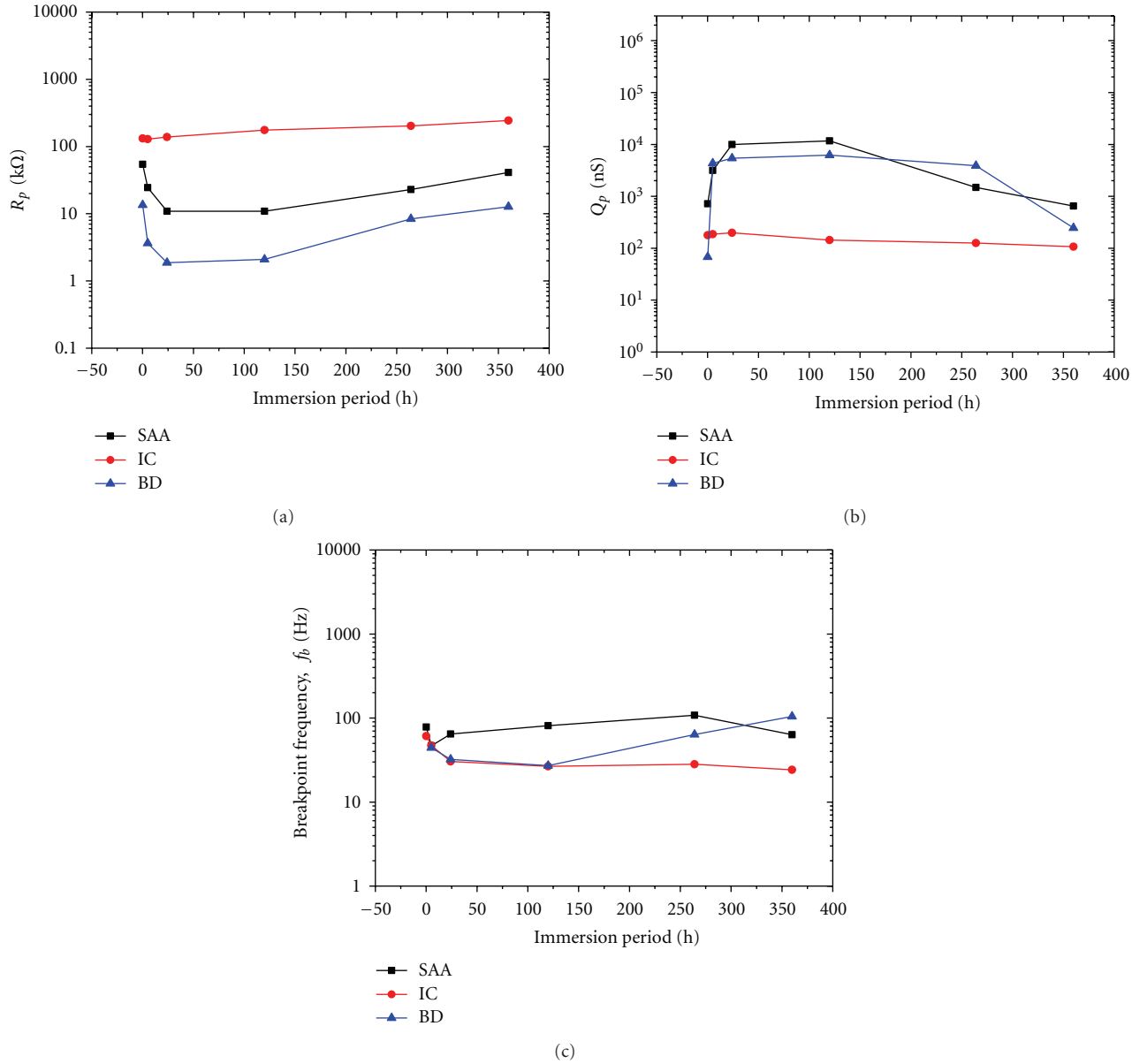

Figure 7: Variation of R_p, Q_p, and f_b over prolonged immersion.

[41]. The disappearance of a quasi-horizontal region in the bode-modulus plot indicates the absence of an electrolyte-filled porous layer which had partly dissolved during the process of electrolytic colouring.

A comparison of the impedance spectra of all coatings shows that the porous layer resistance is found to be higher for IC as compared to SAA and BD. However the capacitive behaviour for porous layer appears to be identical for all three samples that are substantiated by the location of phase-angle minima towards the lower-frequency side for IC. This might be due to the stability of the inorganic pigments which render higher resistance to the porous layer compared to other techniques. From the spectra it can also be concluded that EC follows an entirely different colouring mechanism resulting in a unique electrochemical behaviour of the coating.

Fresh anodic and black anodic coatings gain more corrosion-protective nature by aging [39]. To appraise this property the impedance spectra of black anodized samples (fresh and aged for six months) were studied and presented in Figure 5. These values were compared with the accelerated hydrothermal sealing process, and the results were shown in Figure 5(a). The impedance spectra for fresh-anodized and black-anodized specimens show single straight-line region for the entire frequency range. This could be attributed to the absence of a porous layer resistance in unsealed specimens. Hydrothermal sealing process produces a layered structure consisting of an outer crystalline layer and intermediate hydrated oxide layer followed by partially sealed porous layer filled with sealing solution and a compact barrier layer. This partially filled porous layer has a lower corrosion resistance

due to the presence of water which then increases by the formation of hydrated alumina by aging as discussed earlier in this section. The presence of the horizontal resistive plateau for sealed anodic films is an assertion to the presence of the partially sealed porous layer. The fresh-anodized and black-anodized films generally lack this well-defined hydrated alumina in the porous layer and thus do not give a porous layer resistance to corrosion. Unsealed samples sometimes exhibit a false porous layer resistance as can be seen in Figure 5(a) which could be due to presence of water from atmosphere trapped inside the porous layer which is higher than the freshly sealed as the latter contains more water content. However, fresh-anodized and black-anodized films also develop porous layer resistance because of prolonged exposure to electrolyte or humid atmosphere by self-sealing mechanism. This is confirmed by comparing fresh IC and BD samples aged for 6 months with fresh specimens as shown in Figure 5(b). Interestingly, the impedance spectra for both sealed and fresh specimens coloured by EC are identical in nature. This can be attributed to the deposition of nanolayer of metallic tin which further hinders the formation of hydrated alumina. Thus it can be concluded that impedance behaviour of EC specimens are unaffected by the hydrothermal sealing process.

3.2. Fitting of Impedance Data. Impedance data obtained from various experiments were fitted using NOVA 1.4 software. The impedance data has been best fitted with equivalent circuit models as shown in Figures 6(a) and 6(b) where R_{sol}, R_o and R_p represent the resistances offered by the electrolyte solution, the outer intermediate layer and the porous layer, respectively. Q_o, Q_p and Q_b represent the constant phase elements (CPE) corresponding to the non ideal capacitances at the outer intermediate layer, the porous layer, and the barrier layers, respectively. The constant-phase elements are used to account for the irregularities and variations of the properties of various layers. The equivalent circuit was selected based on a physical model as shown in Figure 6(c). The pore wall resistance and capacitance are neglected as it barely allows conduction of ions through it. The barrier layer resistance R_b also was removed taking into consideration the infinitesimal current across the very large resistance. Finally, the simplified circuit as shown in Figure 6(a) was selected which is similar to the equivalent circuits proposed by Suay et al. and Feliu et al. [19, 42]. However the impedance data for EC samples were best fitted to an equivalent circuit shown in Figure 6(b) which is a consequence of a different layer structure observed for EC samples as discussed in Section 3.1.

Equivalent circuit parameters for porous layer for SAA, BD, and IC were calculated for all the experiments, and the results are displayed in Figure 7. R_p values from Figure 7(a) for all the techniques reveal a common trend. In the initial immersion periods a drastic decrease of R_p is observed which reaches a minimum and then gradually increases till the end of immersion period. This variation of R_p value affirms the results from the EIS spectra and could be explained by the pore wall dissolution and self-sealing stages as previously

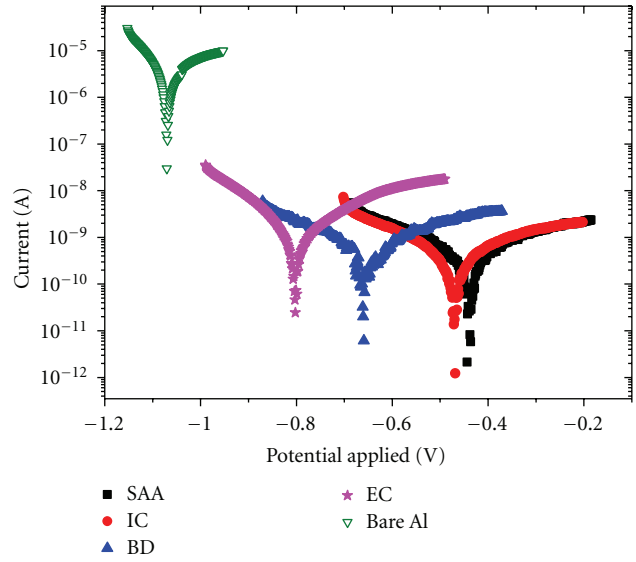

Figure 8: Potentiodynamic polarisation curves for various samples tested in 3.5 wt% NaCl.

Table 2: Damage function (D) analysis for coatings after 360 h of immersion in 3.5 wt% NaCl.

	IC	BD	EC	SAA
D	0.0769	0.0828	0.1251	0.0603

explained. The impedance minima reached after the initial exposure period is attributable to the expansion of the pore diameter [32]. After this stage the self-sealing dominates in which the gel formed by the dissolved anhydrous alumina precipitates to form hydrated alumina. This improves the resistance of the porous layer considerably during aging [33].

Q_p values which represent the CPE of porous layer for various samples over various immersion times are given in Figure 7(b). An increase in the Q_p value in the initial immersion periods up to 24 h is a consequence of the gain of permittivity due to the alumina dissolution from pore walls to the pore volume as the permittivity of water is higher than alumina. Later the saturated pore fillings precipitate as hydrated alumina thus decreasing the permittivity resulting in the decrease of Q_p values during self-sealing [19].

Breakpoint frequency was calculated to find the time dependence of the impedance behaviour of various colouring techniques. F_b values were used to find the variation in the porous layer due to prolonged immersion in corrosive solution [29].

$$\text{Breakpoint frequency is given by } f_b = \frac{1}{2\pi R_p C_p}. \quad (1)$$

Calculated f_b values are shown in Figure 7(c). The f_b values for various colouring samples do not follow a regular trend. For SAA and BD samples slight increase in the f_b was found which could be due to conductive paths or defects developed inside the porous layer during

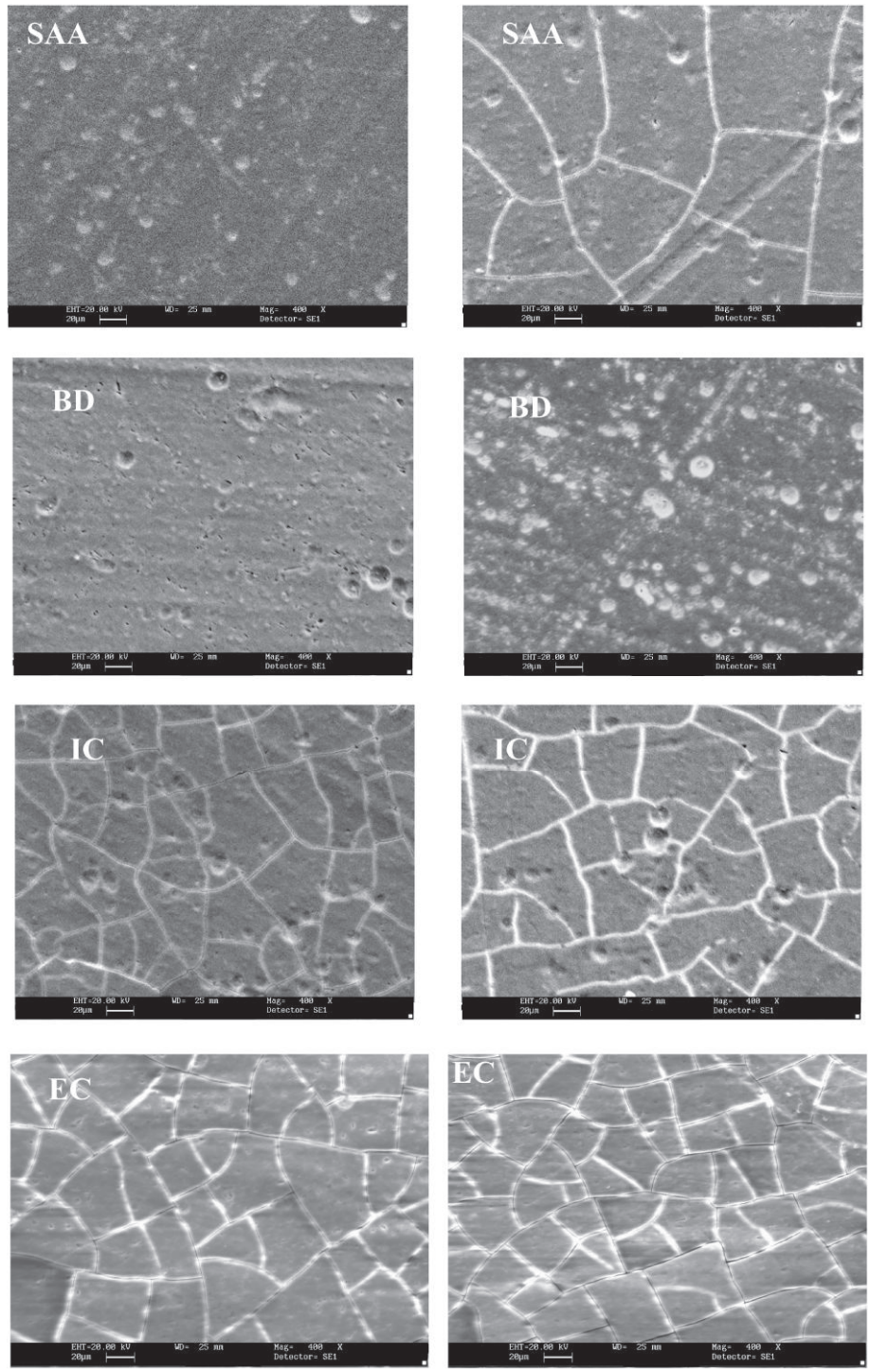

Figure 9: SEM micrographs of anodic and black anodic coatings before and after corrosion.

the exposure period. But the f_b values for IC samples were almost remained constant throughout the immersion period which shows the stability of IC coatings even for prolonged periods of immersion.

Damage function (D) also offers important information in the corrosion behaviour of coatings. It gives a quantitative measure of degradation of impedance modulus over a period of immersion [28]. D is evaluated as follows:

$$D = \log\left(\frac{Z_0}{Z_t}\right)_{0.1\,\text{Hz}}, \tag{2}$$

Table 3: I_{corr} values for various samples after 15 days of exposure.

	β_a (V/dec)	β_c (V/dec)	E_{corr} (V)	I_{corr} (10^{-10} A/cm^2)	R_{Pol} (10^7 Ω/cm^2)
SAA	0.0834	0.0904	−0.4388	6.07	9.40
BD	0.1467	0.1201	−0.6549	6.80	7.12
IC	0.0606	0.0626	−0.4696	3.72	10.3
EC	0.1257	0.0707	−0.8068	13.3	2.50
Bare Al	0.0774	0.1142	−1.0659	61910	0.0007

Where Z_0 and Z_t are impedance modulus values at $t = 0$ and $t = 360$ h, respectively. A zero D value represents a perfect corrosion resistance, and an increase in D value shows decrease in corrosion resistance. The calculated D values are shown in Table 2. SAA shows the least damage after the extended immersion of 360 h in 3.5 wt% NaCl among all coatings though all coatings show very low D values.

3.3. Linear Polarisation. Figure 8 shows polarisation curves of SAA, BC, IC, and EC coloured aluminium samples in 3.5 wt% sodium chloride solution. Compared with bare aluminium alloy (−1.066 V versus SCE), the corrosion potential of the anodised and black-anodized samples increased to −0.439 V versus SCE. This increase represents a positive electrode potential being achieved, thus indicating the improvement of corrosion resistance of aluminium 6061 alloy by carrying out anodizing and black anodizing.

Corrosion current, I_{Corr}, is calculated from anodic and cathodic Tafel slopes from the linear polarisation plots using the Stern-Geary equation given below, and results are shown in Table 3:

$$I_{Corr} = \frac{\beta_a \beta_c}{\beta_a + \beta_c} 2.303 R_{pol}, \quad (3)$$

where β_a and β_c are cathodic and anodic Tafel slopes, respectively, and R_{pol} is the polarisation resistance expressed in $\Omega \cdot cm^2$.

There is no significant difference in the I_{Corr} values of various samples although inorganic colouring showed the least corrosion current value. The calculated polarisation resistance values were also found to be in the same order for all samples showing only slight differences in resistances. So it is concluded that though there are variations in porous layer resistances, no significant difference in the corrosion resistances is noted of various colouring techniques.

3.4. Scanning Electron Microscopy. Figure 9 shows SEM micrographs of the surfaces exposed to 3.5 wt% NaCl solution. The surface morphology corresponds to the outer and intermediate layers which have been formed during black colouring and sealing process and do not reveal the typical hexagonal anodic layer structure [19]. No visible evidence of pitting corrosion is found except that the microcracks and voids showed signs of corrosive attack. All the samples were found to be unaffected even after prolonged exposure of 360 h in sodium chloride solution affirming the high corrosion resistance of the anodized coatings.

4. Conclusions

Three types of black anodic coatings, namely, black dyeing (BD), inorganic colouring (IC), and electrolytic colouring (EC) were prepared by conventional type II sulphuric acid anodizing on Al6061 alloys, and the corrosion performance of the porous layer was studied by electrochemical techniques. The important observations are summarized as follows.

(1) The impedance spectra showed typical three regions for BD and IC as similar to a properly sealed anodic oxide layer (SAA). But impedance spectra for EC are found to be consisting of a single straight-line region without a resistive plateau. This was mainly due to the distinctive mechanism of electrolytic colouring of SAA. Also, impedance behaviour of EC samples was found to be unaffected by HTS.

(2) R_p is found to be decreasing in the initial immersion period which reaches a minimum and increases further till the end of exposure. This variation is generally attributed to the mechanism of pore wall dissolution, gel formation, and precipitation of hydrated alumina. However this mechanism cannot explain the variation of R_p of EC as the anodic layer structure is entirely different from other techniques. In this case, the variation in R_p could be basically attributed to the corrosion of the outer thin layer of metallic tin.

(3) R_p values of BD are found to be lower compared to other colouring techniques which are essentially attributed to the instability of black-dye pigments towards corrosive attack.

(4) Linear polarisation studies confirmed that there is no significant difference in the I_{corr} values of various samples although inorganic colouring showed the lowest corrosion current value.

(5) SEM micrographs revealed no major evidence of any localised pitting during prolonged immersion.

References

[1] R. Uma Rani, A. K. Sharma, S. M. Mayanna, H. Bhojraj, and D. R. Bhandari, "Black permanganate conversion coatings on aluminium alloys for thermal control of spacecraft," *Surface Engineering*, vol. 21, no. 3, pp. 198–203, 2005.

[2] A. K. Sharma, H. Bhojraj, V. K. Kaila, and H. Narayanamurthy, "Anodizing and inorganic black coloring of aluminum alloys for space applications," *Metal Finishing*, vol. 95, no. 12, pp. 14–20, 1997.

[3] R. Umarani, Y. Subba Rao, and A. K. Sharma, "Studies on black anodic coatings for spacecraft thermal control applications," *Galvanotechnik*, vol. 102, p. 2182, 2011.

[4] R. Uma Rani and A. K. Sharma, "Studies on black molybdate conversion coatings on aluminum alloys," *Galvanotechnik*, vol. 93, no. 7, pp. 1736–1746, 2002.

[5] A. K. Sharma, H. Bhojaraj, H. Narayanamurthy, and J. Md. Mohideen, "Integral black anodizing on aluminium alloys," *Journal of Spacecraft Technology*, vol. 2, pp. 35–43, 1992.

[6] T. P. Hoar and G. C. Wood, "The sealing of porous anodic oxide films on aluminium," *Electrochimica Acta*, vol. 7, no. 3, pp. 333–353, 1962.

[7] R. C. Spooner and W. J. Forsyth, "X-ray emission spectroscopic study of the sealing of sulphuric acid anodic films on aluminum," *Plating*, vol. 55, pp. 336–340, 1968.

[8] J. P. O'Sullivan, J. A. Hockey, and G. C. Wood, "Infra-red spectroscopic study of anodic alumina films," *Transactions of the Faraday Society*, vol. 65, pp. 535–541, 1969.

[9] G. C. Wood and J. P. O'Sullivan, "Electron-optical examination of sealed anodic alumina films. Surface and interior effects," *Journal of the Electrochemical Society*, vol. 116, no. 10, pp. 1351–1357, 1969.

[10] Y. Xu, G. E. Thompson, and G. C. Wood, "Direct observation of the cell material comprising porous anodic films formed on aluminium," *Electrochimica Acta*, vol. 27, no. 11, pp. 1623–1625, 1982.

[11] G. E. Thompson, R. C. Furneaux, and G. C. Wood, "The morphology of sealed anodic films formed on aluminum in phosphoric acid," *Transactions of the Institute of Metal Finishing*, vol. 53, pp. 97–102, 1975.

[12] R. C. Furneaux and G. C. Wood, "Assessment of acid immersion tests for the sealing of anodized aluminium," *Transactions of the Institute of Metal Finishing*, vol. 60, no. 1, pp. 14–24, 1982.

[13] K. Wefers, "Mechanism of sealing of anodic oxide coatings on aluminium, Part I+II," *Aluminium*, vol. 49, no. 8, pp. 553–561, 1973.

[14] K. Wefers, "Mechanism of sealing of anodic oxide coatings on aluminium," *Aluminium*, vol. 49, no. 9, pp. 622–625, 1973.

[15] J. Hitzig, K. Jüttner, W. J. Lorenz, and W. Paatsch, "AC-impedance measurements on porous aluminium oxide films," *Corrosion Science*, vol. 24, no. 11-12, pp. 945–952, 1984.

[16] J. Hitzig, K. Juttner, and W. J. Lorenz, "Ac-impedance measurements on corroded porous aluminum oxide films," *Journal of the Electrochemical Society*, vol. 133, no. 5, pp. 887–892, 1986.

[17] H. Shih and F. Mansfeld, "A fitting procedure for impedance data of systems with very low corrosion rates," *Corrosion Science*, vol. 29, no. 10, pp. 1235–1240, 1989.

[18] F. Mansfeld and M. W. Kendig, "Evaluation of anodized aluminum surfaces with electrochemical impedance spectroscopy," *Journal of the Electrochemical Society*, vol. 135, no. 4, pp. 828–833, 1988.

[19] J. J. Suay, E. Giménez, T. Rodríguez, K. Habbib, and J. J. Saura, "Characterization of anodized and sealed aluminium by EIS," *Corrosion Science*, vol. 45, no. 3, pp. 611–624, 2003.

[20] J.-P. Dasquet, D. Caillard, E. Conforto, J.-P. Bonino, and R. Bes, "Investigation of the anodic oxide layer on 1050 and 2024T3 aluminum alloys by electron microscopy and electrochemical impedance spectroscopy," *Thin Solid Films*, vol. 371, no. 1, pp. 183–190, 2000.

[21] V. Lopez, J. A. Gonzalez, E. Otero, E. Escudero, and M. Morcillo, "Atmospheric corrosion of bare and anodised aluminium in a wide range of environmental conditions. Part II: electrochemical responses," *Surface and Coatings Technology*, vol. 153, no. 2-3, pp. 235–244, 2002.

[22] J. A. Gonzalez, V. Lopez, A. Bautista, and E. Otero, "Characterization of porous aluminium oxide films from a.c. impedance measurements," *Journal of Applied Electrochemistry*, vol. 29, no. 2, pp. 229–238, 1999.

[23] M. J. Bartolome, J. F. del Rio, E. Escudero et al., "Behaviour of different bare and anodised aluminium alloys in the atmosphere," *Surface and Coatings Technology*, vol. 202, no. 12, pp. 2783–2793, 2008.

[24] Y. Huang, H. Shih, H. Huang et al., "Evaluation of the corrosion resistance of anodized aluminum 6061 using electrochemical impedance spectroscopy (EIS)," *Corrosion Science*, vol. 50, no. 12, pp. 3569–3575, 2008.

[25] Y. Huang, H. Shih, H. Huang et al., "Evaluation of the properties of anodized aluminum 6061 subjected to thermal cycling treatment using electrochemical impedance spectroscopy (EIS)," *Corrosion Science*, vol. 51, no. 10, pp. 2493–2501, 2009.

[26] F. Snogan, C. Blanc, G. Mankowski, and N. Pébère, "Characterisation of sealed anodic films on 7050 T74 and 2214 T6 aluminium alloys," *Surface and Coatings Technology*, vol. 154, no. 1, pp. 94–103, 2002.

[27] V. Moutarlier, M. P. Gigandet, B. Normand, and J. Pagetti, "EIS characterisation of anodic films formed on 2024 aluminium alloy, in sulphuric acid containing molybdate or permanganate species," *Corrosion Science*, vol. 47, no. 4, pp. 937–951, 2005.

[28] C. Shivakumar, V. Shankar Rao, V. S. Raja, A. K. Sharma, and S. M. Mayanna, "Corrosion behaviour of solar reflector coatings on AA 2024T3—an electrochemical impedance spectroscopy study," *Corrosion Science*, vol. 44, no. 3, pp. 387–393, 2002.

[29] F. Mansfeld and C. H. Tsai, "Determination of coating deterioration with EIS. I. Basic relationships," *Corrosion*, vol. 47, no. 12, pp. 958–963, 1991.

[30] F. Mansfeld, M. W. Kendig, and S. Tsai, "Evaluation of corrosion behavior of coated metals with ac impedance measurements," *Corrosion*, vol. 38, no. 9, pp. 478–485, 1982.

[31] V. Lopez, E. Otero, E. Escudero, and J. A. Gonzalez, "Nanostructural changes in porous anodic films on aluminum during aging," *Surface and Coatings Technology*, vol. 154, no. 1, pp. 34–41, 2002.

[32] V. Lopez, M. J. Bartalome, E. Escudero, E. Otero, and J. A. Gonzalez, "Comparison by SEM, TEM, and EIS of hydrothermally sealed and cold sealed aluminum anodic oxides," *Journal of the Electrochemical Society*, vol. 153, no. 3, pp. B75–B82, 2006.

[33] J. A. Gonzalez and V. Lopez, "Postsealing changes in porous aluminum oxide films obtained in sulfuric acid solutions," *Journal of the Electrochemical Society*, vol. 147, no. 3, pp. 984–990, 2000.

[34] K. Bonnel, C. Le Pen, and N. Pebere, "E.I.S. Characterization of protective coatings on aluminium alloys," *Electrochimica Acta*, vol. 44, no. 24, pp. 4259–4267, 1999.

[35] E. Otero, V. Lopez, and J. A. Gonzalez, "Aging of cold-sealed aluminum-oxide films at room-temperature and at

50-degrees-C," *Plating and Surface Finishing*, vol. 83, no. 8, pp. 50–54, 1996.

[36] J. A. Gonzalez, E. Otero, A. Bautista, and V. Lopez, "Effect of triethanolamine addition on sealing time," *Plating and Surface Finishing*, vol. 84, no. 7, pp. 59–63, 1997.

[37] F. Mansfeld, G. Zhang, and C. Chen, "Evaluation of sealing methods for anodized aluminum alloys with electrochemical impedance spectroscopy (EIS)," *Plating and Surface Finishing*, vol. 84, p. 72, 1997.

[38] Y. Zuo, P.-H. Zhao, and J.-M. Zhao, "The influences of sealing methods on corrosion behavior of anodized aluminum alloys in NaCl solutions," *Surface and Coatings Technology*, vol. 166, no. 2-3, pp. 237–242, 2003.

[39] X.-H. Zhao, Y. Zuo, J.-M. Zhao, J.-P. Xiong, and Y.-M. Tang, "A study on the self-sealing process of anodic films on aluminum by EIS," *Surface and Coatings Technology*, vol. 200, no. 24, pp. 6846–6853, 2006.

[40] I. Tsangaraki-Kaplanoglou, S. Theohari, Th. Dimogerontakis et al., "An investigation of electrolytic coloring process of anodized aluminum coatings," *Surface and Coatings Technology*, vol. 201, no. 6, pp. 2749–2759, 2006.

[41] M. F. Shaffei, N. N. El-Ebiary, M. M. Badran, and G. G. Murad, "Electrolytic colouring of anodized aluminium: a kinetic study," *Metal Finising*, vol. 88, pp. 29–31, 1990.

[42] S. Feliu Jr., J. A. Gonzalez, V. Lopez, M. J. Bartalomem, E. Escudero, and E. Otero, "Characterisation of porous and barrier layers of anodic oxides on different aluminium alloys," *Journal of Applied Electrochemistry*, vol. 37, no. 9, pp. 1027–1037, 2007.